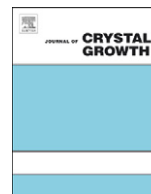




ELSEVIER

Contents lists available at ScienceDirect

Journal of Crystal Growth

journal homepage: www.elsevier.com/locate/jcrysgro

Material characteristics of InGaN based light emitting diodes grown on porous Si substrates

Dongmei Deng^a, Ching-Hsueh Chiu^b, Hao-Chung Kuo^b, Peng Chen^a, Kei May Lau^{a,*}

^a Photonics Technology Center, Department of Electronic and Computer Engineering, Hong Kong University of Science and Technology, Clear Water Bay, Kowloon, Hong Kong, China

^b Department of Photonics and Institute of Electro-Optical Engineering, National Chiao Tung University, Hsinchu, Taiwan, Republic of China

ARTICLE INFO

Available online 17 September 2010

Keywords:

A1. Atomic force microscopy
A1. High resolution X-ray diffraction
A3. Metalorganic chemical vapor deposition
B1. Nitride
B2. Semiconductor III–V materials
B3. Light emitting diode

ABSTRACT

InGaN/GaN multiple quantum wells light emitting diodes (LEDs) with 2 μm thick crack-free GaN buffer layers were grown on porous Si substrates by metalorganic chemical vapor deposition. The material properties of LEDs grown on porous Si were studied in comparison with LEDs grown on grid-patterned Si. The (10 $\bar{1}$ 5) asymmetric reciprocal space mapping (RSM) results indicate that LEDs grown on porous Si have less lattice tilt or distortion than those grown on grid-patterned Si. Both RSM and micro-photoluminescence (micro-PL) measurements suggest that multiple quantum wells grown on porous Si are less stressed. Mechanisms behind this partial strain relaxation are discussed.

© 2010 Elsevier B.V. All rights reserved.

1. Introduction

With the advantages of low cost, large scale availability, and good thermal/electrical conductivities [1,2], Si substrates are promising for growing InGaN based light emitting diodes (LEDs). However, compared with the growth on sapphire or silicon-carbide substrates, it is difficult to obtain high-quality GaN on a Si substrate without cracks. The lattice mismatch between GaN and Si is 17% [3,4], which causes a high dislocation density in the GaN layers. Also, the thermal expansion coefficients of GaN and Si are $5.59 \times 10^{-6} \text{ K}^{-1}$ [5] and $3.59 \times 10^{-6} \text{ K}^{-1}$ [6], respectively, a mismatch of 56%. Stress management between the epi-layers and the substrate during and after the growth is thus of critical importance. The epi-layers are under a large tensile stress during the cooling down process, causing cracks. The cracks in turn degrade both the material property and device performance. To overcome these challenges, epitaxial lateral overgrowth (ELO) [7] and selective area growth (SAG) [8] techniques were proposed and practiced. However, when ELO is implemented at the microscale, a rather thick film needs to be grown to get a fully coalesced surface. Using the SAG technique, accumulated tensile stress can be relieved to a certain extent, but the crystal quality cannot be improved.

Recently, we reported InGaN based LEDs grown and fabricated on nanoscale patterned porous Si substrates [9]. Our results show that nanoscale ELO is significantly promoted on porous Si, leading to extensive dislocation bending and annihilation. LEDs grown on porous Si have lower leakage current and higher light output

power, as compared to those grown on Si substrates with a microscale pattern (grid-pattern). In this work, the material properties of LED structures grown on porous Si substrates are investigated with high resolution X-ray diffraction (XRD), micro-photoluminescence (micro-PL), atomic force microscopy (AFM), and transmission electron microscopy (TEM) techniques, to evaluate the strain profiles of the LED structures on porous Si substrates.

2. Experimental procedures

Two types of substrates were used in this study: one is 2 in. porous Si (1 1 1) substrate and the other is 2 in. grid-patterned Si (1 1 1) substrate. The porous Si substrates were fabricated using the anodized aluminum oxide (AAO) mask patterned at nanoscale, which is a low cost and high throughput approach. Irregular patterns can be obtained by this technique. Detailed information on the preparation of the porous Si substrates can be found in our previous publication [9]. The porous Si substrates used in this work were patterned with an average hole diameter of 150 nm, a spacing of 120 nm, and a depth of 250 nm. For the grid-patterned substrates, the patterns were 340 μm × 340 μm square islands, separated by 3 μm deep and 20 μm wide trenches along the $\langle 1\bar{1}0 \rangle$ and $\langle 11\bar{2} \rangle$ crystalline orientations as shown in Ref. [10].

InGaN based LED structures were grown by MOCVD in an Aixtron 2000HT system. Trimethylgallium (TMGa), trimethylaluminum (TMAI), trimethylindium (TMIn), and ammonia were used as sources for Ga, Al, In, and N, respectively. Triethylgallium (TEGa) was used as the precursor for InGaN quantum wells growth instead of TMGa. SiH₄ and bis(cyclopentadienyl)magnesium

* Corresponding author. Tel.: +852 23587049; fax: +852 23581485.
E-mail address: eekmlau@ust.hk (K.M. Lau).

(CP₂Mg) were used as n-type and p-type doping sources, respectively. Prior to the growth, substrates were heated up to 1170 °C for 10 min under an H₂ ambient to remove the native oxide on the surface of Si substrates. For growth on porous Si, an AlN seed layer (~40 nm) was first deposited, followed by growth of a 200 nm thick AlGa_xN layer and 800 nm thick undoped GaN layer. For growth on grid-patterned Si, the AlN seed layer (~30 nm) was followed by a SiN_x in-situ nanomask layer. Subsequently, an 800 nm thick undoped GaN buffer layer was deposited. In these two samples, AlN/AlGa_xN interlayers (~125 nm thick) were deposited after the growth of the undoped GaN layer, which aimed to further reduce the tensile stress. For comparison purpose, the same LED structures were grown on porous Si and grid-patterned Si substrates. The LED structure consisted of a 1 μm thick Si doped GaN layer, five periods of InGa_xN/GaN multiple quantum wells (MQWs), a 20 nm thick Mg doped AlGa_xN electron blocking layer and a 150 nm thick Mg doped GaN layer. Both samples were crack-free after growth. High resolution XRD measurements were performed using a wavelength of 0.15406 nm. Excitation power dependent micro-PL was carried out using a 385 nm frequency doubled Ti:sapphire laser. The laser spot diameter was 50 μm, and the excitation power varied from 0.05 to 50 mW.

3. Results and discussion

The crystalline quality and lattice relaxation behavior of samples grown on grid-patterned and porous Si substrates were investigated by asymmetrical (10 $\bar{1}$ 5) reciprocal space mapping (RSM) measurements as shown in Fig. 1. The two maps indicate the intensity distribution (plotted on a logarithmic scale) as a function of deviation from the exact Bragg diffraction condition. H and L are the scattering vector components in units of $2\pi/a_{\text{GaN}}$ and $2\pi/c_{\text{GaN}}$, respectively [11]. The insets in Fig. 1(a) and (b) show the optical microscope and scanning electron microscope (SEM) images of grid-patterned and porous Si substrates, respectively, the LEDs were grown on. The intensity scale is the same in these two maps (i.e. a maximum intensity contour of $10^{0.54}$ and a minimum contour level of $10^{-0.8}$). In each map, the main peak is from the underlying GaN, and the satellite peaks are from the MQWs. Widths of the peaks of GaN in both H and L directions are relatively small in Fig. 1(b), where the growth was performed on porous Si, as compared to Fig. 1(a), where growth was performed on grid-patterned Si. This indicates that the lattice tilt or distortion of GaN grown on porous Si is smaller than that of GaN grown on grid-patterned Si. In Fig. 1(a), the perpendicular

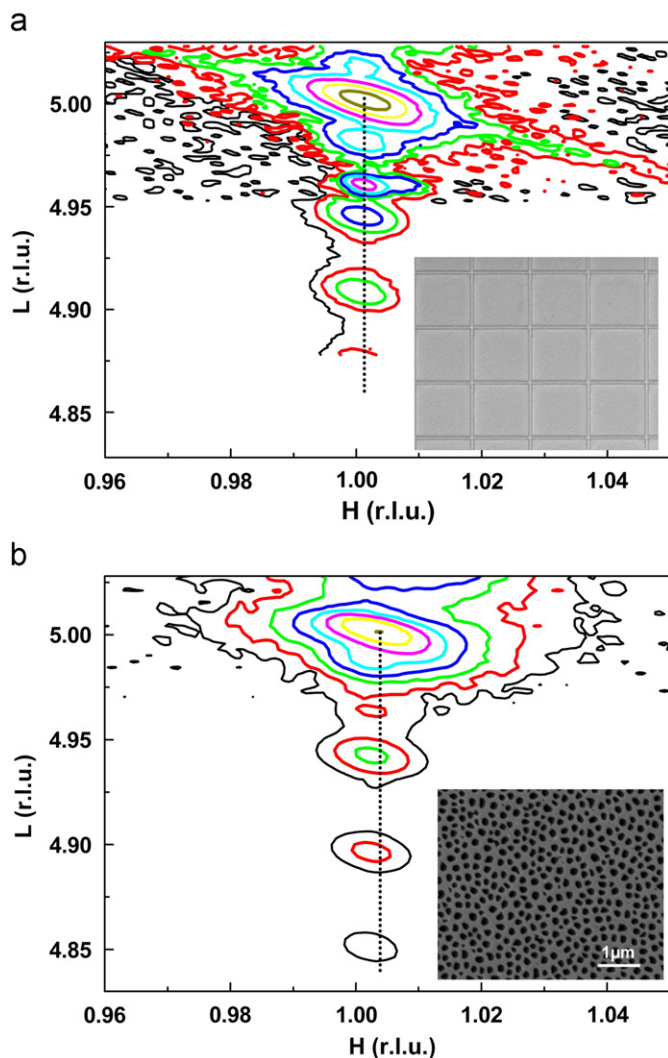


Fig. 1. RSM around (10 $\bar{1}$ 5) diffraction plane of LEDs grown on grid-patterned Si substrate (a) and porous Si substrate (b). Insets show the SEM images of porous Si (a) and grid-patterned Si (b). The two maps have the same intensity scale. Dotted lines are guide to the eye.

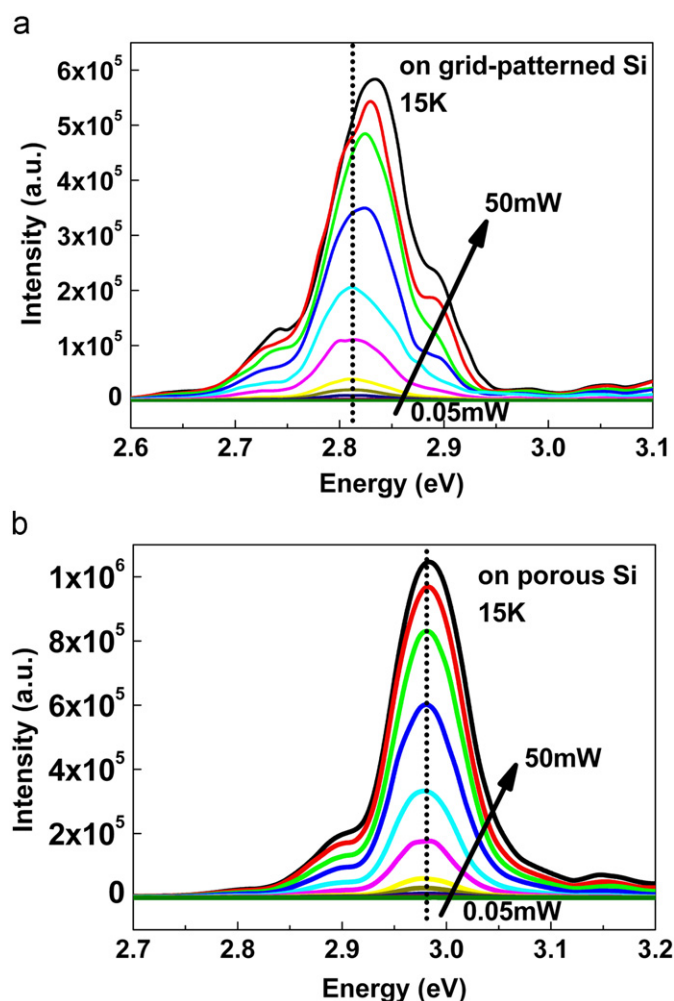


Fig. 2. Excitation power dependent micro-PL spectra of LEDs grown on grid-patterned (a) and porous (b) Si substrates. Measurements were carried out at 15 K. Excitation power increased from 0.05 to 50 mW. Dotted lines are guide to the eye; (a) and (b) used the same set of arbitrary unit, so the PL intensity can be compared.

dotted line goes through all the peak centers, suggesting a fully strained structure. However, the MQW peaks in Fig. 1(b) deviate from the GaN peak in H direction, which suggests the MQWs grown on porous Si are slightly relaxed. In each map, the slight right shift of the GaN peak position from the stress-free diffraction condition ($H=1$) indicates that the in-plane lattice constant of the GaN layer is somewhat smaller than the value at a stress-free condition ($a=3.189 \text{ \AA}$). However, based on our previous results, the GaN layers on porous and grid-patterned Si are under tensile stress [9]. It appears that the RSM results are not in agreement with the micro-Raman data, which were previously used to determine the stress. However, Romano et al. [12] have reported a similar phenomenon, i.e., when the GaN layer is under increasing tensile stress, the change in the in-plane lattice constant is still negligible. The explanation for this observation is not clear at this point.

Excitation power dependent micro-PL measurements were carried out at low temperature (15 K) to study the strain conditions of the MQWs. Usually, the InGaN layers are under compressive strain in the MQWs. This compressive strain induces a piezoelectric field, which in turn bends the energy band and decreases the overlap of electron and hole wave functions, thus reducing the MQW internal efficiency. When the sample is under excitation, the injected electron–hole pairs will screen the strain-induced piezoelectric field and relieve the band bending. With increase in excitation power, the peak position of micro-PL gradually shifts to higher energies as shown in Fig. 2(a), because of partial cancellation of quantum confinement stark effect. In Fig. 2(b), no obvious peak position shift was observed, which suggests the MQWs grown on porous Si are less strained. This observation is consistent with the RSM results. In Fig. 2(b), the feature on the low-energy side of the main peak may be due to the phonon replica of the main peak [13], but this is not the focus of this work. In Fig. 2(a), the shoulders are likely caused by an interference phenomenon, since these shoulders have roughly the same distance from the main peak ($\sim 0.09 \text{ eV}$). The two samples were measured under the same experimental conditions, so it is reasonable to compare the PL intensities of the two samples at the same temperature and same excitation power. From Fig. 2, it is obvious that the LEDs grown on porous Si substrate have much stronger emission intensity. Moreover, the PL full width at half maximum (FWHM) of LEDs on porous Si and on grid-patterned Si are 80 and 90 meV at 50 mW excitation, respectively. This indicates that LEDs on porous Si have better crystal quality.

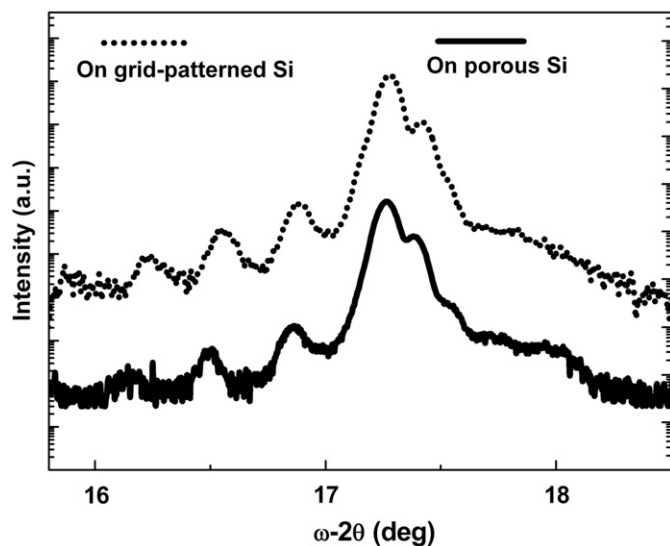


Fig. 3. The (002) ω - 2θ curve of LEDs grown on porous (solid line) and grid-patterned (dot line) Si substrates.

To further investigate the possible reasons for the different states of strain in these two samples, high resolution XRD (002) ω - 2θ scans were employed to evaluate the MQW structures. As can be seen in Fig. 3, the average In fractions are slightly different in two samples. The average In incorporation has been reported to be influenced by the strain in GaN buffer layer, which may play a role in PL emission energy [14].

The surface morphologies of GaN layers underneath the MQWs were studied. AFM was used for characterizing the surface morphology of GaN grown on grid-patterned and porous Si substrates, shown in Fig. 4(a) and (b). The AFM scan area is $10 \mu\text{m} \times 10 \mu\text{m}$. The surface roughness root mean square (RMS) values obtained from AFM measurements were 4.6 and 2.6 nm for the GaN buffer grown on porous and grid-patterned Si, respectively. From the surface roughness data, one can tell that the buffer layer grown on porous Si has a rougher surface than that grown on grid-patterned Si. It has been reported that the strain in InGaN layers could be relieved by introducing a rough GaN

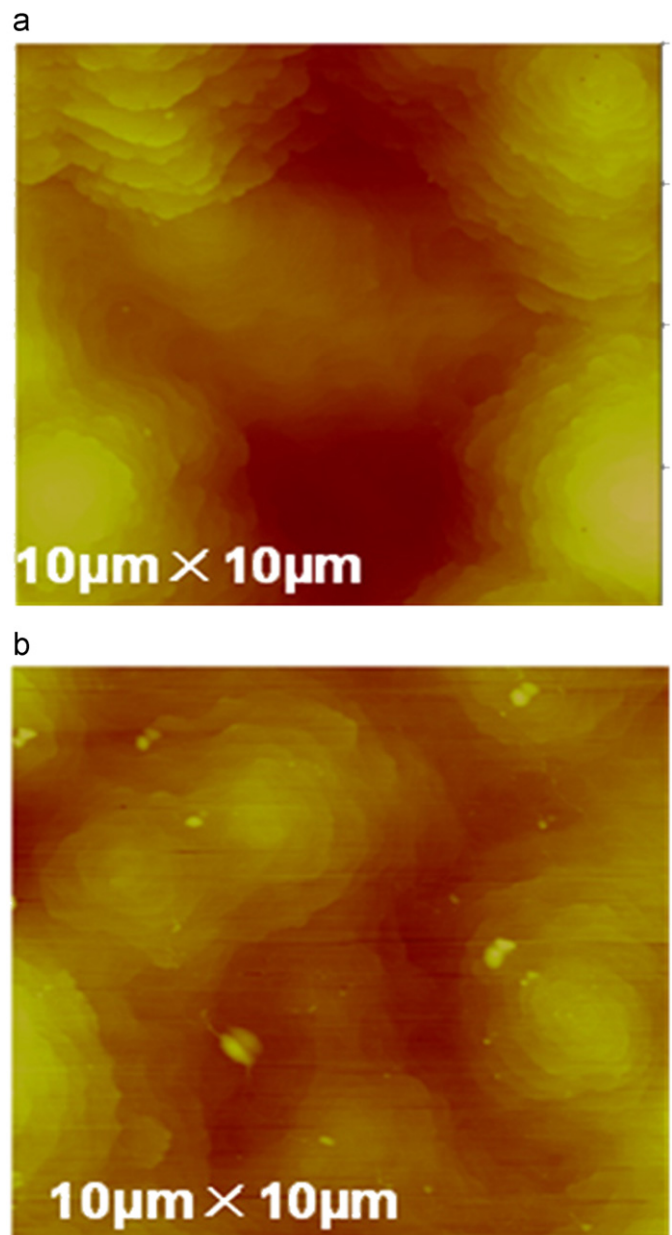


Fig. 4. AFM images of GaN buffers grown on grid-patterned (a) and porous Si (b) substrates. The image size is $10 \mu\text{m} \times 10 \mu\text{m}$.

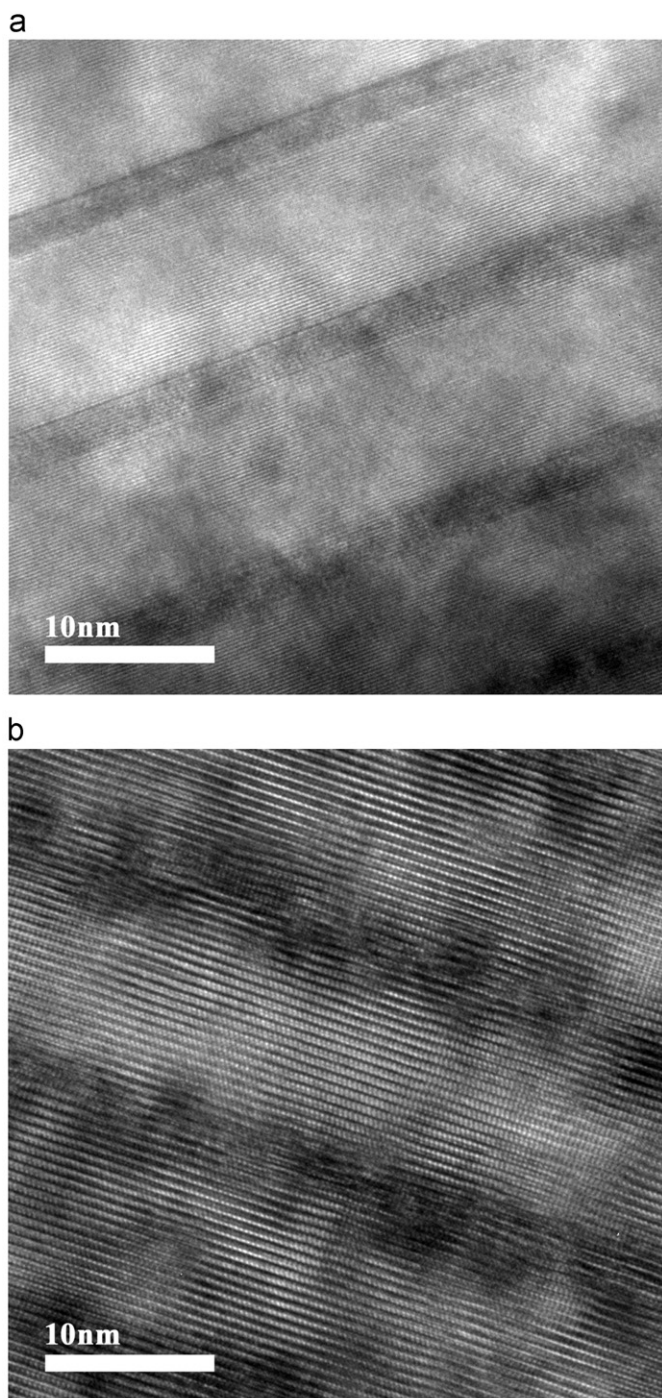


Fig. 5. TEM images of the MQWs grown on grid-patterned Si (a) and porous Si (b) substrates.

surface as an underlying layer [15]. From the simulated XRD (002) ω - 2θ results and the TEM images (shown in Fig. 5), the InGaN well thickness is around 2 nm. Compared with the 4.6 nm roughness of the GaN layer on porous Si, the InGaN layer may not exist as a 2-dimensional (2-D) film, but as 3-D disk-like or island-like In-rich dots. This is confirmed by the TEM results. Compared with Fig. 5(a), numerous dark spots are observed across the well in Fig. 5(b). The dark spots in the TEM image can be attributed to In-rich dots [16]. The 3-D nature of these dots would enable the generation of misfit dislocations, which may relieve the lattice mismatch strain in the InGaN layer [17]. It may be the possible

reason for strain relaxation in LEDs grown on porous Si substrates. The exact mechanism for relaxation still needs further study.

4. Summary

Material characteristics of LEDs grown on porous and grid-patterned Si substrates were analyzed by various techniques. Asymmetric RSM and PL results indicate that LEDs grown on porous Si have better crystal quality in the GaN buffer with a narrower width of peak in RSM and PL. Micro-PL results suggest that the MQWs grown on porous Si have less piezoelectric field, which is consistent with the RSM observations. From XRD ω - 2θ scans, AFM and TEM images, the strain relaxation in MQWs grown on porous Si substrates is believed to be mainly caused by the 3-D In dots induced misfit dislocations.

Acknowledgments

The authors would like to thank Prof. Chunlei Yang, Dr. Xueliang Zhu, and Dr. Zhen-Yu Li for the valuable discussion on this work. The research work was supported in part by a grant (615705) from the Research Grants Council and a grant (GHP/034/07GD) from the Innovation and Technology Commission (ITC) of Hong Kong Special Administrative Government (HKSAR).

References

- [1] B. Gil, in: Group III Nitride Semiconductor Compounds—Physics and Application, Oxford University Press, New York, 1998.
- [2] S. Nakamura, G. Fasol, in: The Blue Laser Diode: GaN Based Light Emitters and Lasers, Springer, New York, 1997.
- [3] M. Leszczynski, T. Suski, H. Teisseyre, P. Perlin, I. Grzegory, J. Jun, S. Porowski, T.D. Moustakas, Thermal expansion of gallium nitride, *J. Appl. Phys.* 76 (1994) 4909–4911.
- [4] W.M. Yim, R.J. Paff, Thermal expansion of AlN, sapphire and silicon, *J. Appl. Phys.* 45 (1974) 1456–1457.
- [5] W. Qian, M. Skowronski, G.R. Rohrer, Structural defects and their relationship to nucleation of GaN thin films, in: D.K. Gaskill, C.D. Brandt, R.J. Nemanich (Eds.), III-Nitride, SiC, and Diamond Materials for Electronic Devices, Mat. Res. Soc. Symp. Proc., Pittsburgh, PA, 1996, 423 pp. 475–486.
- [6] Y. Okada, Y. Tokumaru, Precise determination of lattice parameter and thermal expansion coefficient of silicon between 300 and 1500 K, *J. Appl. Phys.* 56 (1984) 314–320.
- [7] M. Seon, T. Prokofyeva, M. Holtz, Selective growth of high quality GaN on Si(111) substrates, *Appl. Phys. Lett.* 76 (2000) 1842–1844.
- [8] S. Tanaka, Y. Honda, N. Sawaki, Structural characterization of GaN laterally overgrown on a (111) Si substrate, *Appl. Phys. Lett.* 79 (2001) 955–957.
- [9] D.M. Deng, N.S. Yu, Y. Wang, X.B. Zou, H.C. Kuo, P. Chen, K.M. Lau, InGaN-based light-emitting diodes grown and fabricated on nanopatterned Si substrates, *Appl. Phys. Lett.* 96 (2010) 201106: 1–3.
- [10] B.S. Zhang, H. Liang, Y. Wang, Z.H. Feng, K.W. Ng, K.M. Lau, High-performance III-nitride blue LEDs grown and fabricated on patterned Si substrates, *J. Cryst. Growth* 298 (2007) 725–730.
- [11] O. Thomas, Q. Shen, P. Schieffer, N. Tournerie, B. Lépine, Interplay between anisotropic strain relaxation and uniaxial interface magnetic anisotropy in epitaxial Fe films on (001) GaAs, *Phys. Rev. Lett.* 90 (2003) 017205: 1–4.
- [12] L.T. Romano, C.G. Van de Walle, J.W. Ager, W. Götz, R.S. Kern, Effect of Si doping on strain, cracking, and microstructure in GaN thin films grown by metalorganic chemical vapor deposition, *J. Appl. Phys.* 87 (2000) 7745–7752.
- [13] T. Wang, G. Raviprakash, F. Ranalli, C.N. Harrison, J. Bai, J.P.R. David, P.J. Parbrook, Effect of strain relaxation and exciton localization on performance of 350-nm AlInGaN quaternary light-emitting diodes, *J. Appl. Phys.* 97 (2005) 083104: 1–4.
- [14] A. Dadgar, J. Christen, T. Riemann, S. Richter, J. Bläsing, A. Diez, A. Krost, A. Alam, M. Heuken, Bright blue electroluminescence from a InGaN/GaN multiquantum-well diode on Si (111): impact of an AlGaIn/GaN multilayer, *Appl. Phys. Lett.* 78 (2001) 2211–2213.
- [15] I.K. Park, M.K. Kwon, S.H. Baek, Y.W. Ok, T.Y. Seong, S.J. Park, Y.S. Kim, Y.T. Moon, D.J. Kim, Enhancement of phase separation in the InGaN layer for self-assembled In-rich quantum dots, *Appl. Phys. Lett.* 87 (2005) 061906: 1–3.
- [16] D.J. Kim, Y.T. Moon, K.M. Song, C.J. Choi, Y.W. Ok, T.Y. Seong, S.J. Park, Structural and optical properties of InGaIn/GaN multiple quantum wells: the effect of the number of InGaIn/GaN pairs, *J. Cryst. Growth* 221 (2002) 368–372.
- [17] C.G. Tuppen, C.J. Gibbings, A quantitative analysis of strain relaxation by misfit dislocation grid in $\text{Si}_{1-x}\text{Ge}_x/\text{Si}$ heterostructures, *J. Appl. Phys.* 68 (1990) 1526–1534.